

Investigate small particles with unparalleled sensitivity  
**Amnis® CellStream®** Flow Cytometry System

For Research Use Only. Not for use in diagnostic procedures.



**Luminex®**  
complexity simplified.



## Differing Activities of Homeostatic Chemokines CCL19, CCL21, and CXCL12 in Lymphocyte and Dendritic Cell Recruitment and Lymphoid Neogenesis

This information is current as of August 9, 2022.

Sanjiv A. Luther, Afshin Bidgol, Diana C. Hargreaves, Andrea Schmidt, Ying Xu, Jyothi Paniyadi, Mehrdad Matloubian and Jason G. Cyster

*J Immunol* 2002; 169:424-433; ;  
doi: 10.4049/jimmunol.169.1.424  
<http://www.jimmunol.org/content/169/1/424>

**References** This article cites **65 articles**, 34 of which you can access for free at:  
<http://www.jimmunol.org/content/169/1/424.full#ref-list-1>

**Why *The JI*? Submit online.**

- **Rapid Reviews! 30 days\*** from submission to initial decision
- **No Triage!** Every submission reviewed by practicing scientists
- **Fast Publication!** 4 weeks from acceptance to publication

*\*average*

**Subscription** Information about subscribing to *The Journal of Immunology* is online at:  
<http://jimmunol.org/subscription>

**Permissions** Submit copyright permission requests at:  
<http://www.aai.org/About/Publications/JI/copyright.html>

**Email Alerts** Receive free email-alerts when new articles cite this article. Sign up at:  
<http://jimmunol.org/alerts>

*The Journal of Immunology* is published twice each month by  
The American Association of Immunologists, Inc.,  
1451 Rockville Pike, Suite 650, Rockville, MD 20852  
Copyright © 2002 by The American Association of  
Immunologists All rights reserved.  
Print ISSN: 0022-1767 Online ISSN: 1550-6606.



# Differing Activities of Homeostatic Chemokines CCL19, CCL21, and CXCL12 in Lymphocyte and Dendritic Cell Recruitment and Lymphoid Neogenesis<sup>1</sup>

Sanjiv A. Luther, Afshin Bidgol,<sup>2</sup> Diana C. Hargreaves,<sup>2</sup> Andrea Schmidt, Ying Xu, Jyothi Paniyadi, Mehrdad Matloubian, and Jason G. Cyster<sup>3</sup>

Despite their widespread expression, the *in vivo* recruitment activities of CCL19 (EBV-induced molecule 1 ligand chemokine) and CXCL12 (stromal cell-derived factor 1) have not been established. Furthermore, although CXCL13 (B lymphocyte chemoattractant) has been shown to induce lymphoid neogenesis through induction of lymphotoxin (LT) $\alpha$ 1 $\beta$ 2, it is unclear whether other homeostatic chemokines have this property. In this work we show that ectopic expression in pancreatic islets of CCL19 leads to small infiltrates composed of lymphocytes and dendritic cells and containing high endothelial venules and stromal cells. Ectopic CXCL12 induced small infiltrates containing few T cells but enriched in dendritic cells, B cells, and plasma cells. Comparison of CCL19 transgenic mice with mice expressing CCL21 (secondary lymphoid tissue chemokine) revealed that CCL21 induced larger and more organized infiltrates. A more significant role for CCL21 is also suggested in lymphoid tissues, as CCL21 protein was found to be present in lymph nodes and spleen at much higher concentrations than CCL19. CCL19 and CCL21 but not CXCL12 induced LT $\alpha$ 1 $\beta$ 2 expression on naive CD4 T cells, and treatment of CCL21 transgenic mice with LT $\beta$ R-Fc antagonized development of organized lymphoid structures. LT $\alpha$ 1 $\beta$ 2 was also induced on naive T cells by the cytokines IL-4 and IL-7. These studies establish that CCL19 and CXCL12 are sufficient to mediate cell recruitment *in vivo* and they indicate that LT $\alpha$ 1 $\beta$ 2 may function downstream of CCL21, CCL19, and IL-2 family cytokines in normal and pathological lymphoid tissue development. *The Journal of Immunology*, 2002, 169: 424–433.

Secondary lymphoid organs are critical for bringing APCs and lymphocytes together for initiating adaptive immune responses, and animals that lack these organs are strongly immunocompromised (1, 2). Lymphoid tissue also frequently forms at sites of inflammation, especially in chronic autoimmune diseases, such as in the pancreas of diabetics and in the joint synovium of rheumatoid arthritis patients, and the local development of lymphoid tissue is thought to contribute to pathology (3, 4). More recently, induction of ectopic lymphoid tissue has been considered as an approach to the immunotherapy of cancer (3).

Lymphoid tissue organization is promoted by a subset of the chemokine family, sometimes called homeostatic or lymphoid chemokines because of their constitutive expression in preformed lymphoid tissues (5, 6). These include CXCL13 (B lymphocyte chemoattractant), the ligand of CXCR5; CCL19 (EBV-induced molecule 1 ligand chemokine) and CCL21 (secondary lymphoid tissue chemokine), ligands for CCR7; and CXCL12 (stromal cell-derived factor 1), the ligand of CXCR4 (7). CXCL13 is made by

stromal cells in B cell follicles and is required for homing of B cells to the follicular compartment (8). Expression of CXCL13 in pancreatic islets of transgenic mice was found not only to cause B cell recruitment but also to lead to development of ectopic lymph node-like structures containing T cell areas, with high endothelial venules (HEVs)<sup>4</sup> and stromal cells (9). Development of these structures was dependent on signaling by lymphotoxin (LT) $\alpha$ 1 $\beta$ 2. These observations indicated that CXCL13 could activate a LT-dependent process of lymphoid neogenesis (9). Naive B cells have been shown to be an important source of LT $\alpha$ 1 $\beta$ 2 and more recently it was established that CXCL13 can up-regulate LT $\alpha$ 1 $\beta$ 2 on B cells (8, 10). Activated T cells and NK cells can also express LT $\alpha$ 1 $\beta$ 2 (11, 12). Studies in CXCR5-deficient and CXCL13-deficient mice have confirmed that these molecules are important in the development of many secondary lymphoid organs (8, 13), and LT $\alpha$ 1 $\beta$ 2 and its receptor, LT $\beta$ R, are also critical for normal development of all secondary lymphoid organs (10).

CCR7 and its ligands function to guide naive T cells and maturing dendritic cells (DC) into T zones of secondary lymphoid organs (6). CCL19 and CCL21 are both constitutively expressed by stromal cells within lymphoid T zones and CCL21 is expressed by HEVs and, at lower levels, by lymphatic endothelium (14–16). In addition to stromal cells, CCL19 expression is found in DCs (16–20). Recent evidence suggests that CCL19 protein can be translocated onto the lumen of HEVs (21). *In vitro*, CCL19 and CCL21 induce chemotaxis of mature DCs, naive and activated T

Howard Hughes Medical Institute and Department of Microbiology and Immunology, University of California, San Francisco, CA 94143

Received for publication February 20, 2002. Accepted for publication April 16, 2002.

The costs of publication of this article were defrayed in part by the payment of page charges. This article must therefore be hereby marked *advertisement* in accordance with 18 U.S.C. Section 1734 solely to indicate this fact.

<sup>1</sup> This work was supported by National Institutes of Health Grant AI 45073, a Packard Fellowship, and the Howard Hughes Medical Institute. S.A.L. was supported in part by a Human Frontier Science Program fellowship. M.M. was supported by a Pfizer postdoctoral fellowship grant in Immunology/Rheumatology and the Rosalind Russell Medical Research Center for Arthritis.

<sup>2</sup> A.B. and D.C.H. contributed equally to this work.

<sup>3</sup> Address correspondence and reprint requests to Dr. Jason G. Cyster, Department of Microbiology and Immunology, University of California, 513 Parnassus Avenue, San Francisco, CA 94143-0414. E-mail address: cyster@itsa.ucsf.edu

<sup>4</sup> Abbreviations used in this paper: HEV, high endothelial venule; NOD, nonobese diabetic; DC, dendritic cell; LT, lymphotoxin; Ptx, pertussis toxin; PNAd, peripheral lymph node addressin; MAdCAM, mucosal addressin cell adhesion molecule; RIP, rat insulin promoter; HPRT, hypoxanthine phosphoribosyltransferase.

cells, and, to a lesser degree, B cells. Furthermore, ectopic expression of CCL21 in the pancreatic islets was sufficient to cause infiltration by T cells, B cells, and DCs as well as to induce HEVs (22, 23). However, to what extent these effects reflect the direct action of CCL21 vs induction of downstream events was not clear, and the relative *in vivo* activities of CCL19 and CCL21 remain unknown. Both CCL19 and CCL21 have been found to be up-regulated at sites of chronic inflammation (24–29).

The CXCL12/CXCR4 ligand/receptor pair is critical in bone marrow hematopoiesis and plays important roles in gut vasculogenesis and heart and brain development, and deficiency in either the receptor or the ligand causes perinatal lethality (Ref. 30 and references therein). Consistent with these diverse functions, CXCL12 (stromal cell-derived factor 1) is expressed broadly, including expression by stromal cells within bone marrow and in many epithelial tissues. Within secondary lymphoid tissues, there is expression in the splenic red pulp, in lymph node medullary cords, and in the subepithelial region of tonsil (31, 32). *In vitro*, CXCL12 is a chemoattractant for naive B cells and T cells as well as DCs and plasma cells (Refs. 30 and 31 and references therein). Recently, CXCR4-deficient plasma cells were shown to localize aberrantly in the spleen and failed to accumulate appropriately in the bone marrow (31). CXCL12 is strongly up-regulated in the joint synovium of rheumatoid arthritis patients and may also contribute to skin inflammatory responses (33–35).

The strong *in vitro* chemotactic activities of CCL19, CCL21, and CXCL12 for T cells and DCs, together with their frequent expression at sites of inflammation, led us to generate transgenic mice to examine the *in vivo* chemotactic and nonchemotactic functions of these chemokines. Using the rat insulin promoter (RIP) system (36), we demonstrate that all three chemokines are able to induce lymphoid structures within the pancreas, but we find that these structures show striking differences in size, cellular composition, and organization. The differences are shown to correlate with chemokine protein concentration and the propensity to induce LT $\alpha$ 1 $\beta$ 2 on naive T cells. We also show that members of the IL-2 cytokine family induce LT $\alpha$ 1 $\beta$ 2 expression on naive T cells and suggest that they also may activate a LT $\alpha$ 1 $\beta$ 2-dependent pathway of lymphoid tissue formation. These results have implications for our understanding of lymphoid tissue organization, chronic inflammatory responses, and lymphomagenesis.

## Materials and Methods

### Mice

To generate transgenic mice, the full-length cDNA of murine CCL19, CCL21-leu (CCL21b), and CXCL12 was cloned into a *Clal* site of the 10-kb RIP7 promoter construct (9). Linearized constructs were injected into B6D2F1 oocytes and transgenic mice backcrossed to C57BL/6 for one to five generations. Seven lines of RIP-CCL19 (transgene copy number estimated as 12 and 76 for lines I and II, respectively), three lines of RIP-CCL21 (13, three, and eight copies for lines I, II, and IV, respectively), and four lines of RIP-CXCL12 (34, 31, nine, and one copy for lines I, II, III, and IV, respectively) were established and characterized. Homogenous expression in all  $\beta$  cells was obtained with all mouse lines except RIP-CCL21 line IV and RIP-CXCL12 line I, where expression was restricted to a small subset of  $\beta$  cells. Most results presented were obtained with RIP-CCL19 line II, RIP-CCL21 line II, and RIP-CXCL12 line II. RIP-CXCL13 mice have been previously described (9). None of the transgenic mouse strains developed obvious symptoms of diabetes. Mice were screened by PCR using the following primers: 5'-CAACCCTGACTA TCTCCAG (RIP7, forward), 5'-GAGATGATAGTGGCTTCAGGCAG-3' (CXCL13, reverse), 5'-CTACTAATCGATCCAGAGTGATTCACATC TC-3' (CCL19, reverse), 5'-CTACTAATCGATGGACCGTGAACCAC CCAG-3' (CCL21, reverse), or 5'-TAGTAGATCGATGCTCTTGGGCT GTTGTGC-3' (CXCL12, reverse). Some adult RIP-CCL21 mice received *i.p.* injections of 100  $\mu$ g soluble human LFA3-Fc or murine LT $\beta$ R-Fc fusion protein (kindly provided by J. Browning, Biogen, Cambridge, MA) two times a week as previously described (37). Tissues were harvested

after 20 days. Nonobese diabetic (NOD) females were from Jackson ImmunoResearch Laboratories (West Grove, PA).

### Immunohistochemistry

Mice were euthanized with CO<sub>2</sub> and tissues were removed and frozen in OCT compound (Miles, Elkhart, IN). Cryostat sections (10  $\mu$ m) were collected on Superfrost plus slides (Fisher Scientific, Pittsburgh, PA), dried overnight, fixed for 10 min in acetone (4°C), and stained with reagents and procedures described previously (9). Chemokine stainings were done in four steps: blocking with 0.1% BSA and 4% normal mouse and donkey serum, application of polyclonal goat sera to CCL19, CCL21 (R&D Systems, Minneapolis, MN), or CXCL12 (Santa Cruz Biotechnology, Santa Cruz, CA), followed by donkey anti-goat IgG (Jackson ImmunoResearch Laboratories) and streptavidin-ABC (Vector Laboratories, Burlingame, CA). Plasma cells were detected using a rat anti-mouse IgM-biotin (Caltag Laboratories, Burlingame, CA) followed by streptavidin-AP (Vector Laboratories).

### Quantification of histology

Every fifteenth 10- $\mu$ m section from the pancreas was counterstained with hematoxylin and the number of islets and the number of mononuclear cells per islet were counted. Infiltrates were scored as small (5–30 cells), medium (31–300 cells), and large (>300 cells). Islets with fewer than five mononuclear cells were scored as noninfiltrated. This procedure was applied for 80–160 islets per pancreas.

### Western blot analysis

Whole spleen or a pool of mesenteric and peripheral lymph nodes was homogenized in ice-cold lysis buffer (120 mM NaCl, 50 mM Tris-HCl (pH 8), 1 mM EDTA, 6 mM EGTA, 1% Nonidet P-40) containing protease inhibitors (1 mM PMSF, 1 mM benzimidazole, 1  $\mu$ g/ml leupeptin, and 1  $\mu$ g/ml aprotinin). For pancreas, the protease inhibitor TLCK was also added at 50  $\mu$ g/ml. Debris was removed by centrifugation and supernatant was either used as whole lysate or immunoprecipitated using heparin-Sepharose as previously described (16). Detection was with goat anti-mouse CCL19, CCL21, CXCL13 (R&D Systems), or CXCL12 (Santa Cruz Biotechnology) followed by anti-goat HRP (Jackson ImmunoResearch Laboratories); development was with ECL Plus (Amersham Pharmacia Biotech, Piscataway, NJ). Specificity was controlled by showing lack of reactivity of the CCL19-, CCL21-, and CXCL13-specific Abs with lysates from CCL19/CCL21-deficient (*plt/plt*) mice (16, 38) or CXCL13-deficient mice (8). Titrations of recombinant chemokines (R&D Systems) were used to quantify the amount of chemokines in tissues. Concentrations of chemokines in tissues was calculated by dividing the amount of chemokine per total tissue with the average weight for pancreas (90 mg), spleen (90 mg), and pooled lymph nodes (40 mg).

### Quantitative RT-PCR analysis

PCR primers and probes for CCL19, CCL21, and hypoxanthine phosphoribosyltransferase (HPRT) were as previously described (16). CCL19 primers were specific for the functional CCL19 transcript (CCL19-atg), with a new 3' primer (5'-cttcgcatcattagacc-3'). The CCL21 primers detect total CCL21 transcript levels and do not distinguish between CCL21-ser (CCL21a) and CCL21-leu (CCL21b) transcripts (39). Quantitative RT-PCR was performed on an ABI 7700 sequence detection instrument (TaqMan; PE Applied Biosystems, Foster City, CA) following the manufacturer's instructions. The relative efficiency of CCL19 and CCL21 mRNA amplification was established using various amounts of expressed sequence tag plasmids encoding CCL19-atg (clone AA444730) or CCL21-ser (clone AW987545.1). After correction for the difference in amplification efficiency the expression of CCL19 and CCL21 in mRNA samples was quantified using HPRT as a reference. The specificity of the primers used to amplify CCL19 and CCL21 have previously been controlled by showing a >4000-fold lower amplification in samples from *plt* compared with wild-type mice (16). Lymph node pool was composed of mesenteric and peripheral nodes.

### *In vitro* LT $\alpha$ 1 $\beta$ 2 induction and flow cytometry

Spleen cell suspensions were prepared, RBCs were lysed, and cells were preincubated for 14–17 h in flat-bottom 96-well plates and complete RPMI medium containing 10% FCS to allow adjustment to *in vitro* conditions. For pretreatment with pertussis toxin (Ptx), cells were incubated for 2 h with 200 ng/ml toxin. The indicated concentration of recombinant chemokines or cytokines (R&D Systems) was added for 6 h at 37°C. Cells were placed on ice, washed, and stained for surface LT $\alpha$ 1 $\beta$ 2 using LT $\beta$ R-Fc fusion protein (37). In brief, cells were pretreated with FcR blocking Ab



(2.4.G2; BD PharMingen, San Diego, CA), 0.5% normal mouse and rat serum, and, if indicated, anti-LT $\beta$  blocking Ab (BBF6). LT $\beta$ R-Fc was added and detected using either F(ab')<sub>2</sub> goat anti-human Ig-PE (Jackson ImmunoResearch Laboratories) or biotinylated goat anti-human IgG (Jackson ImmunoResearch Laboratories), both of which were pretreated for 30 min with 4% normal mouse and rat serum. Finally, FITC-conjugated anti-CD69 (BD PharMingen), PE-conjugated anti-CD4 and anti-CD8 (Caltag Laboratories), PerCP-conjugated anti-B220 (BD PharMingen), and streptavidin-allophycocyanin were added (Molecular Probes, Eugene, OR). Cells were analyzed using a four-color FACSCalibur (BD Biosciences, Mountain View, CA) and FlowJo software (BD Biosciences).

## Results

### *Ectopic expression of CCL21 and CCL19 in islets induces lymphoid tissue*

To study the *in vivo* activities of CCL21 and CCL19, a total of three lines of RIP-CCL21 and seven lines of RIP-CCL19 transgenic mice were established and characterized. Histological analysis of pancreas tissue from each of the transgenic mouse lines showed detectable chemokine protein expression within  $\beta$  cells of pancreatic islets (Fig. 1A and data not shown). Nontransgenic pancreas showed a low level of CCL21 expression that was limited to

lymphatic endothelium, as previously reported (9), and no detectable CCL19 (data not shown). Pancreatic islets of RIP-CCL21 transgenic mice were often infiltrated by large numbers of CD4<sup>+</sup> and CD8<sup>+</sup> T cells, IgD<sup>+</sup> B cells, and CD11c<sup>+</sup> DCs (Fig. 1A), confirming two previous reports on independently generated RIP-CCL21 transgenic mouse lines (22, 23). No evidence for infiltration by Mac-1<sup>+</sup> or MOMA-1<sup>+</sup> macrophages was obtained. Interestingly, CCL19 induced fewer and smaller infiltrates that were often associated with large blood vessels (Fig. 1A). This observation is representative for all seven RIP-CCL19 transgenic lines. These small cellular accumulations were rare in young mice and increased in frequency in older animals (Fig. 2A; see also Fig. 4C). Flow cytometric analysis of infiltrates in pancreas of old RIP-CCL19 and RIP-CCL21 mice showed a similar composition, with B cells representing the largest population and CD4 T cells being more frequent than CD8 T cells (Fig. 2B). Although CCL19 was sufficient to attract the same cell types as CCL21, CCL19-induced infiltrates were less organized, with T cells, B cells, and DCs frequently being interspersed (Fig. 1A). Besides attracting various hematopoietic cell types, both chemokines were sufficient to cause development of HEVs, characterized by thick endothelium and expression of peripheral lymph node addressin (PNAd) and mucosal addressin cell adhesion molecule (MAdCAM) (Fig. 1B and data not shown). Surprisingly, CCL21 and CCL19 protein were not detected on HEVs within the infiltrate of the respective mouse lines (Fig. 1A and data not shown). Both chemokines also caused variable but reproducible appearance of gp38<sup>+</sup>, BP3<sup>+</sup>, and ER-TR7<sup>+</sup> stromal cell networks within the infiltrates (Fig. 1B and data not shown). Consistent with the larger infiltrate size and more defined organization of T and B zones, CCL21 showed a higher efficiency than CCL19 in inducing HEVs and stromal cell networks (Fig. 1B). Neither of the two mouse models showed evidence for development of CD35<sup>+</sup> follicular DCs or CXCL13-expressing stromal cells (data not shown).

A striking feature of the infiltrates in RIP-CCL21 transgenic mice was the localization of DCs and T cells, but not B cells, close to the chemokine-expressing islet cells. Exactly the opposing pattern has been previously observed in RIP-CXCL13 transgenic mice (9), where B cells line the islets and T cells are localized more distantly (Fig. 2C). Another important difference between the infiltrates induced by CCR7 and CXCR5 ligands was that CCL21, and to a lesser degree CCL19, induced infiltrates showing an invasive phenotype with a ragged boundary between accumulating T cells and islet cells and the frequent presence of individual T cells within the islet cell mass (Fig. 2C and data not shown). This intraislet invasion was only rarely observed in RIP-CXCL13 transgenic mice, where large numbers of B cells are found to accumulate next to clusters of islet cells without mixing of islet cells and lymphocytes (Fig. 2C). An analysis of the autoimmune infiltrates that form in islets of NOD mice has previously shown the presence of CCL21 transcripts (26). By immunohistochemistry, we were able to detect CCL21 protein on vessels and stromal cells within infiltrates of prediabetic NOD mice (Fig. 2D). A fraction of the infiltrates in NOD mice shows intraislet invasiveness (40), a feature possibly important in islet cell destruction. However, no signs of diabetes were observed in RIP-CCL21 or RIP-CCL19 transgenic animals up to 12 mo of age, establishing that chemokine-mediated islet invasion by T cells is not sufficient to cause disease.

To examine whether CCL19 and CCL21 may function in a synergistic manner in promoting ectopic lymphoid tissue development, we generated mice coexpressing CCL19 and CCL21 by intercrossing RIP-CCL19 and RIP-CCL21 transgenic mice. No increase of infiltrate size in double transgenic compared with CCL21 single transgenic mice was detected by hematoxylin staining

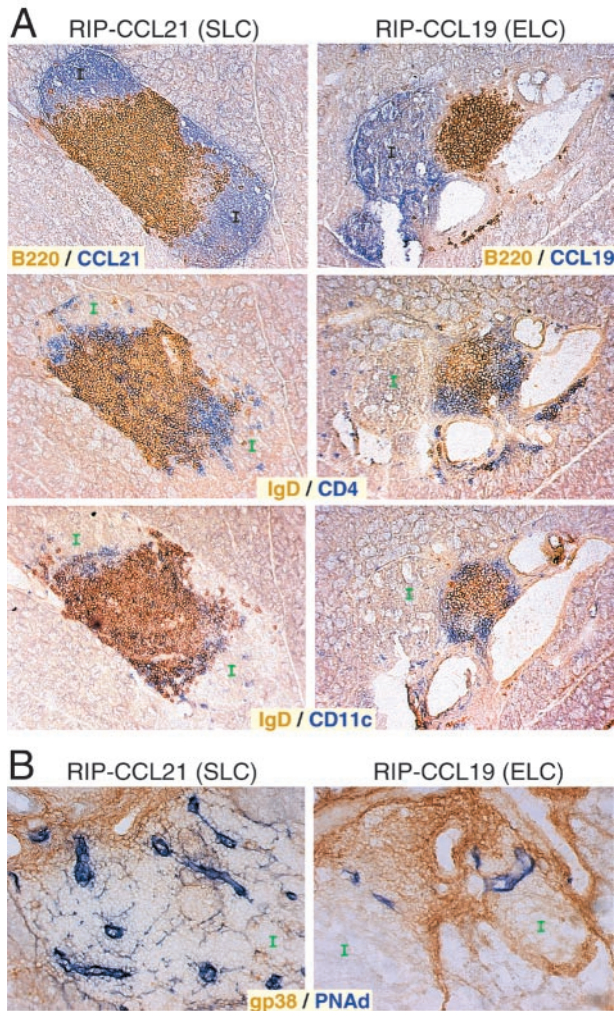


**FIGURE 1.** Histological comparison of pancreatic infiltrates in RIP-CCL21 and RIP-CCL19 transgenic mice. Shown is immunohistochemistry on adjacent pancreatic sections from either RIP-CCL21 or RIP-CCL19 mice stained in brown for B220, IgD, or gp38 and in blue for CCL21, CCL19, CD4, CD11c, or PNAd, as indicated on each micrograph. I, Islet. Objective magnification was  $\times 10$ , except for gp38/PNAd-stained sections, in which magnification was  $\times 20$ .



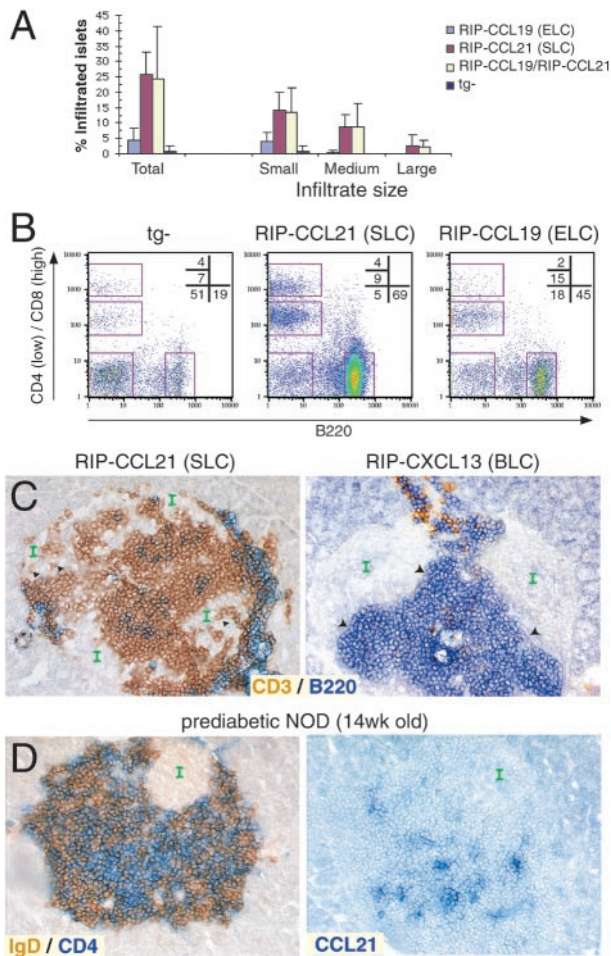


**FIGURE 2.** Analysis of the size, composition, and invasiveness of infiltrates in RIP-CCL21 and RIP-CCL19 transgenic mice and detection of CCL21 protein in infiltrates of prediabetic NOD mice. *A*, Quantitative analysis of infiltrate frequency in pancreatic sections from RIP-CCL19 ( $n = 7$ ) and RIP-CCL21 ( $n = 7$ ) single transgenic, RIP-CCL19/CCL21 ( $n = 5$ ) double transgenic, and nontransgenic littermate (tg<sup>-</sup>) mice ( $n = 4$ ) at 2–3.5 mo of age. *B*, Representative flow cytometric analysis of infiltrates found in the pancreas of nontransgenic (tg<sup>-</sup>) littermate, RIP-CCL21, and RIP-CCL19 transgenic mice. Lymphocytes were isolated from perfused pancreas of 12- to 18-mo-old mice and stained with B220, CD4, and CD8. CD4 and CD8 were stained with the same fluorophore and are identified by their low (CD4) or high (CD8) fluorescence intensity. Numbers in the *top right* of each profile indicate the percentage of total cells within the corresponding gate. The average number of lymphocytes isolated from three pancreases of either nontransgenic, RIP-CCL21, or RIP-CCL19 transgenic mice was 90,000, 450,000, and 270,000, respectively. *C*, An example of invasive features of islet infiltrates in RIP-CCL21 mice. Sections of RIP-CCL21 and RIP-CXCL13 pancreas stained for CD3 (brown) and B220 (blue). Arrowheads in *left panel* show small intraislet T cell clusters in RIP-CCL21 mice. Arrows in *right panel* highlight the tight boundary between islet cells and B cells in RIP-CXCL13 mice. *D*, CCL21 expression in insulinitis of NOD mice. Shown is immunohistochemistry on adjacent pancreatic sections from a 14-wk-old female NOD mouse, stained in brown for IgD and in blue for CD4 or CCL21, as indicated on each micrograph. CCL21 was detected at high levels on structures resembling HEVs and at lower levels within the infiltrates, possibly on stromal cells. Expression of the lymphoid stromal cell markers, gp38 and BP3, was also observed (data not shown). This pattern of CCL21 staining is representative for several infiltrates in two 14-wk-old NOD mice and two 22-wk-old diabetic NOD mice. However, some islet infiltrates did not contain detectable CCL21 expression. A similar analysis for CCL19, CXCL12, and CXCL13 failed to reveal detectable staining. I, Islet. Objective magnification:  $\times 20$ .

(Fig. 2A). Similarly, immunohistochemical analysis showed little difference in the composition and orientation of the pancreatic infiltrates in double vs CCL21 single transgenic mice (data not shown).

#### *Differential expression of CCL21 and CCL19 in transgenic pancreas and secondary lymphoid organs*

To investigate the basis for the differential efficiency of CCL21 vs CCL19 in induction of infiltrates in RIP transgenic mice, we first measured the amount of the respective chemokines present within the pancreas. Western blot of lysates from RIP-CCL21 pancreas revealed large amounts of CCL21 protein (2–20 ng per milligram of pancreas), while the amounts present in nontransgenic pancreas were below detection (Fig. 3, *A* and *D*). Assuming similar detection of endogenously expressed recombinant CCL19, we estimate this chemokine was present only at very low levels (0.01–0.2 ng/mg) in pancreatic lysates from RIP-CCL19 transgenic mice (Fig. 3, *A* and *D*). This  $\sim 100$ -fold difference in CCL19 and CCL21 protein levels was consistently observed in pancreas tissue from mouse lines derived from at least two founders of each type (data not shown). Analysis of chemokine mRNA levels in the two types of transgenic mice by quantitative PCR revealed a difference of  $< 10$ -fold (Fig. 3*E*), consistent with the use of identical promoter and enhancer regions in the transgenic constructs.

We also measured levels of endogenous CCL19 and CCL21 protein in secondary lymphoid organs. Despite similar sensitivities of the polyclonal antisera in detecting the recombinant chemokines, only CCL21 but not CCL19 could be detected in whole tissue lysates from spleen and lymph nodes, indicating at least a 30-fold difference in protein levels (Fig. 3*B*). When chemokines and other basic proteins were enriched from the lysates by precipitation with heparin-Sepharose, CCL19 became detectable (Fig. 3*C*). Our analysis indicates  $> 100$ -fold higher levels of CCL21 protein compared with CCL19 in both spleen and lymph nodes (Fig. 3*D*). By contrast, CCL19 and CCL21 mRNA levels in spleen and lymph nodes differed by  $< 5$ -fold (Fig. 3*F*). Therefore, the large difference in protein levels in lymphoid tissues and in the transgenic system indicates that CCL19 protein accumulates in tissues less efficiently than CCL21 protein. A similar quantitative analysis of CXCL13 in lymphoid organs revealed protein expression levels that are a few fold above CCL19 but  $\sim 50$ -fold lower than CCL21 (Fig. 3, *C* and *D*). These results are consistent with protein staining data on histological sections of secondary lymphoid organs where CCL19 is undetectable and CCL21 is more easily detectable than CXCL13 (Refs. 8, 9, and 16 and data not shown).

#### *Ectopic expression of CXCL12 induces DC and plasma cell accumulation*

Similar to CCL19 and CCL21, CXCL12 attracts T and B cells as well as DCs *in vitro*. To investigate CXCL12 function *in vivo*, RIP-CXCL12 transgenic mice were generated. Expression of CXCL12 in pancreatic islets caused only small, occasional infiltrates to develop, although these became more frequent in older mice (Fig. 4, *A* and *C*). Unlike the small infiltrates in RIP-CCL19 transgenic mice, the CXCL12-induced cell accumulations consisted mainly of naive B cells with only small numbers of T cells. Strikingly, however, the CXCL12-induced infiltrates contained large proportions of DCs and plasma cells (Fig. 4*A*). Plasma cells were only occasionally found in infiltrates of RIP-CCL21 (Fig. 4*B*), RIP-CCL19, and RIP-CXCL13 transgenic mice (data not shown). In some cases, these infiltrates were associated with stromal cell networks and small vessels expressing HEV markers (data not shown). We examined a total of four RIP-CXCL12 mouse lines and found similar infiltrations in a second line, whereas two

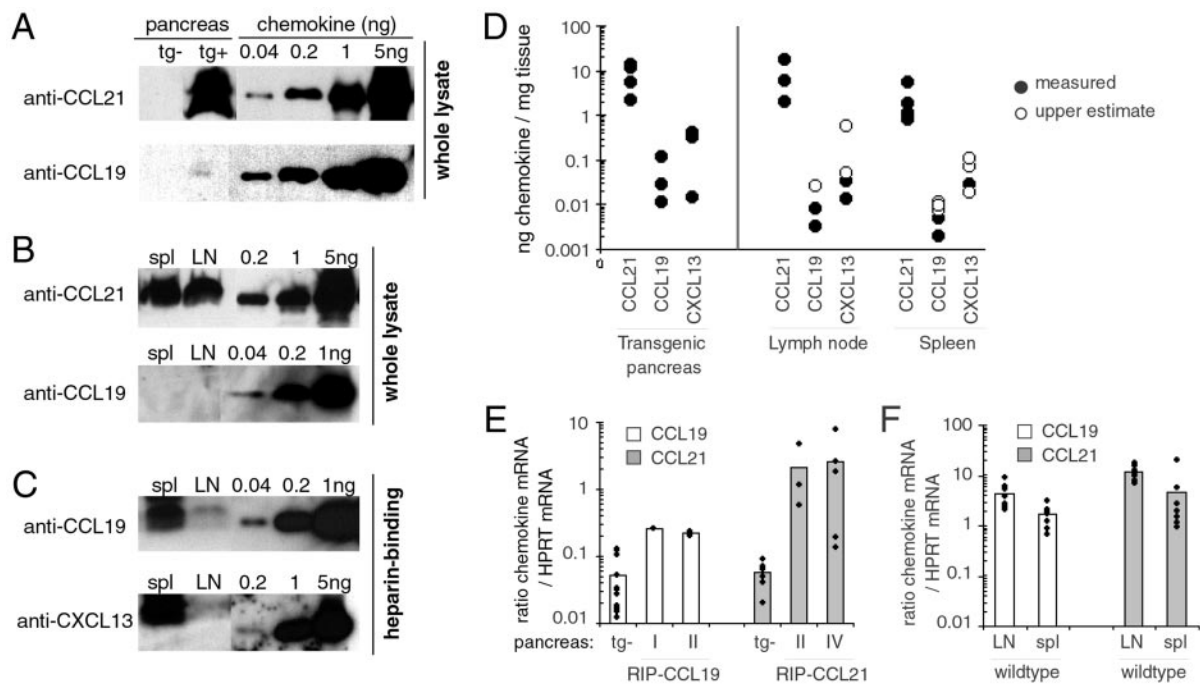


**FIGURE 3.** Quantitative analysis of chemokine expression in transgenic pancreas and in nontransgenic spleen and lymph node. Shown is a Western blot of whole lysate from nontransgenic (tg<sup>-</sup>) and transgenic (tg<sup>+</sup>) pancreas (A), and from wild-type spleen and lymph node (B), showing >100-fold higher expression levels of CCL21 compared with CCL19 in all three organs. Blots include a titration of recombinant chemokines as standard. Loading was as follows: 1/400 of total RIP-CCL21 pancreas, 1/250 of total RIP-CCL19 pancreas, 1/50 of total spleen, 1/25 of lymph node pool. Blots were probed with anti-CCL21 and anti-CCL19 Abs, as indicated. Occasionally, doublet bands were observed for CCL21 and CCL19 in pancreas and lymphoid tissues. C, Heparin precipitates of whole lysates from spleen and lymph node probed with anti-CCL19 or anti-CXCL13 Abs as indicated. Precipitates corresponding to one-fifth of spleen and one-fifth to one-seventh of the lymph node pool were loaded. D, Quantitative assessment of CCL19, CCL21, and CXCL13 protein concentration in nanograms of chemokine per milligram of total tissue, based on a compilation of Western blot data from whole or heparin-precipitated lysates of 8- to 20-wk-old mice. ●, Measurements where a signal was detected within the whole cell lysate or heparin precipitate. ○, Upper limits of the amount of chemokine that could have been present in samples where no signal was detected. E and F, Real-time quantitative RT-PCR analysis of CCL19 and CCL21 mRNA levels relative to HPRT mRNA level in samples from transgenic pancreas (E) or nontransgenic (wild-type) lymph node and spleen (F). A titration analysis with CCL19 and CCL21 plasmid DNA established a 3-fold lower amplification efficiency for CCL19 vs CCL21, and the threshold cycle values obtained for the CCL19 mRNA samples were multiplied by a factor of three to correct for this difference in reaction efficiency. Shown in E are relative chemokine expression levels in nontransgenic (tg<sup>-</sup>) pancreas as well as in RIP-CCL-19 transgenic pancreas from mouse lines I and II and in RIP-CCL21 transgenic pancreas from mouse lines II and IV.

lines showed minimal CXCL12 expression and no detectable infiltration. CXCL12 protein levels in the highest expressing mouse line were estimated to be 1–2 ng chemokine per milligram of pancreas (data not shown). This amount is ~5- to 10-fold below the level of CCL21 in the pancreas of RIP-CCL21 mice, 4- to 8-fold above the level of CXCL13 in RIP-CXCL13 mice, and 10- to 40-fold above the level of CCL19 in RIP-CCL19 mice (Fig. 3D).

Comparing the four lymphoid chemokine transgenic mouse models, only a partial correlation between chemokine expression level and infiltration frequency can be observed. CCL21 and CXCL13 induce a high frequency of infiltrates of all sizes in young mice, while mice expressing CCL19 and CXCL12 only develop small and medium-size infiltrates, and these only become prominent when the animals are more than 4 mo of age (Fig. 4C).

#### Chemokine-mediated $LT\alpha1\beta2$ induction on T cells

In addition to quantity and relative activity in promoting chemotaxis, a further property of chemokines influencing their activity in promoting ectopic lymphoid tissue development is their ability to induce  $LT\alpha1\beta2$  expression (8). Surprisingly, although naive T cells have not been reported to express  $LT\alpha1\beta2$ , we found that CD4 and CD8 T cells from blood constitutively expressed very low amounts of membrane  $LT\alpha1\beta2$  (Fig. 5A). The specificity of  $LT\beta$ -Fc for  $LT\alpha1\beta2$  was confirmed by the lack of staining on

$LT\beta$ -deficient T cells (data not shown) and by the background level of staining in the presence of a  $LT\beta$  blocking Ab (Fig. 5A). In contrast to B cells,  $LT\alpha1\beta2$  expression was not increased on T cells in lymph nodes (Fig. 5A) or spleen (data not shown), suggesting that lymphoid tissue chemokines may not be involved in inducing  $LT\alpha1\beta2$  expression on naive T cells. However, when recombinant CCL21 was added to splenocytes in vitro,  $LT\beta$ -Fc ligands on CD4 T cells were strongly up-regulated within 6 h (Fig. 5B). Addition of an  $LT\beta$  blocking Ab reduced staining to levels equivalent to nontreated cells (Fig. 5B). When splenocytes were pretreated with Ptx before adding CCL21, up-regulation of  $LT\alpha1\beta2$  was prevented, indicating involvement of  $G_i$  protein-coupled signals downstream of CCR7. When other T cell chemoattractants were tested, CCL19 but not CXCL12 induced  $LT\alpha1\beta2$  up-regulation on naive CD4 T cells (Fig. 5B). To compare CD4 and CD8 T cells and B cells for their sensitivity to chemokine-mediated induction of  $LT\alpha1\beta2$ , a titration analysis was performed using all four previously described chemokines. Surprisingly, concentrations as low as 0.1 nM CCL19 and 1 nM CCL21 were sufficient to induce  $LT\alpha1\beta2$  expression on CD4 T cells (Fig. 5C). In contrast, CD8 T cells showed only a very modest induction of  $LT\alpha1\beta2$ , even at high concentrations of CCL19 and CCL21 (Fig. 5D). CXCL12 failed to cause notable  $LT\alpha1\beta2$  expression on T cells (Fig. 5, C and D) but was capable of promoting expression on



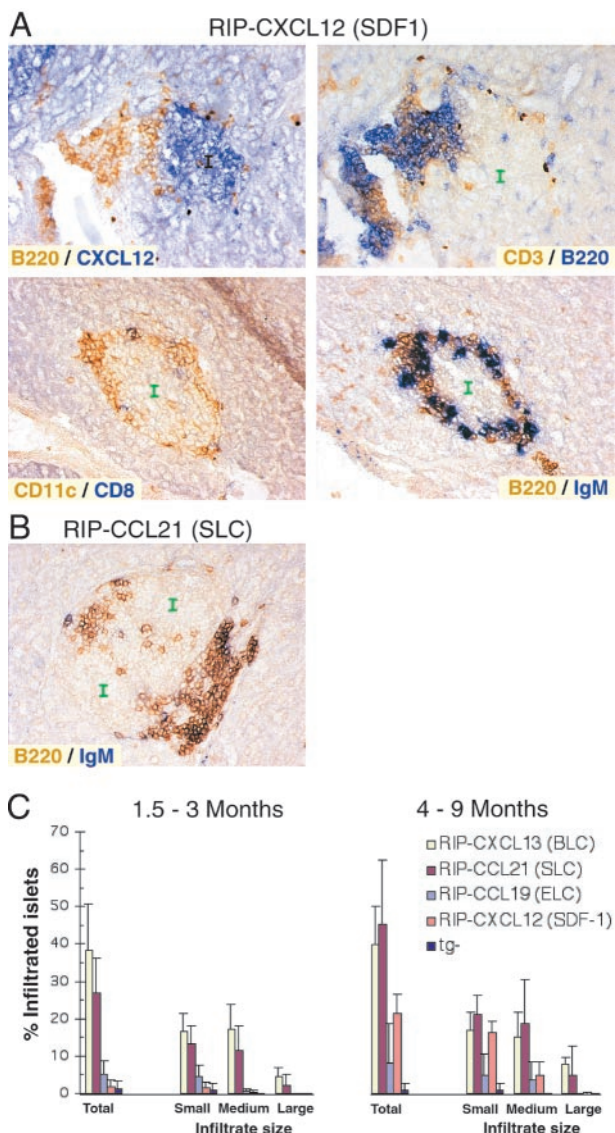


**FIGURE 4.** RIP-CXCL12 transgenic mice develop small pancreatic infiltrates composed of B cells, plasma cells, and DCs. Immunohistochemistry on pancreatic sections from RIP-CXCL12 (A) and RIP-CCL21 (B) transgenic mice, stained in brown for B220, CD3, or CD11c and in blue for CXCL12, B220, CD8, or IgM, as indicated. I, Islet. Sections stained for B220/CXCL12 and CD3/B220 were adjacent sections, as were the sections stained for CD11c/CD8 and B220/IgM. Cells that stain strongly for IgM correspond to plasma cells and weakly stained cells are B cells. Objective magnification:  $\times 20$ . C, Quantitative analysis of infiltrate frequency in pancreatic sections from 1.5- to 3-mo-old and 4- to 9-mo-old RIP-CXCL13 ( $n = 9$  for young mice and 4 for old mice), RIP-CCL21 ( $n = 11$  for young mice and 8 for old mice), RIP-CCL19 ( $n = 6$  for young mice and 7 for old mice), RIP-CXCL12 ( $n = 5$  for young mice and 5 for old mice) transgenic mice, and nontransgenic (tg<sup>-</sup>) littermate mice ( $n = 9$  for young mice and 6 for old mice). The data for 1.5- to 3-mo-old RIP-CCL21 and RIP-CCL19 mice are the same as shown in Fig. 2A and are included here to facilitate comparisons.

B cells (Fig. 5E), as previously observed (8). Interestingly, the concentrations of CXCL13 required for LT $\alpha$ 1 $\beta$ 2 induction on B cells (Fig. 5E) were  $>10$ -fold higher than the amounts of CCL21 needed to promote strong LT $\alpha$ 1 $\beta$ 2 up-regulation on CD4 T cells.

#### LT $\beta$ R-Fc treatment of RIP-CCL21 mice causes loss of HEV and stromal cells

To test whether CCL21-induced pancreatic infiltrates were dependent on signals by the LT $\alpha$ 1 $\beta$ 2-LT $\beta$ R pathway, we treated RIP-

CCL21 transgenic mice for 3 wk with LT $\beta$ R-Fc or with a control protein (hLFA3-Fc). Histological analysis showed only a weak effect of LT $\beta$ R-Fc treatment on infiltrate size, composition, and orientation (Fig. 6A). Strikingly, however, administration of LT $\beta$ R-Fc strongly reduced the expression of the adhesion molecules PNA $\alpha$  and MAdCAM on HEVs within infiltrated islets (Fig. 6B). Filamentous stromal cell networks, identified by gp38, BP3, and PNA $\alpha$  staining, were also greatly affected by this treatment (Fig. 6B). Our attempts to identify the cell population expressing LT $\alpha$ 1 $\beta$ 2 in infiltrates of RIP-CCL21 pancreas were not successful, most likely due to the enzymatic digest required for the isolation of infiltrating cells and the low sensitivity of the detection of surface LT $\alpha$ 1 $\beta$ 2. In summary, in this experimental setting LT $\alpha$ 1 $\beta$ 2 appears to play a specific role downstream of CCL21 that includes the induction or maintenance of activated endothelial cells and stromal cells but not the retention or organization of attracted lymphocytes. The related observations in RIP-CXCL13 transgenic mice (9) suggest that several chemokines can influence the development, growth, or activation of stromal and endothelial cells by regulating LT $\alpha$ 1 $\beta$ 2 expression on lymphocytes. Consistent with this notion is the correlation between the low numbers of stromal cells and addressin-expressing HEVs in RIP-CXCL12 and RIP-CCL19 infiltrates and the relatively weak capacity of these two chemokines to induce LT $\alpha$ 1 $\beta$ 2 in vitro (Fig. 5, B-E).

#### Cytokine-mediated LT $\alpha$ 1 $\beta$ 2 induction on T cells

Previous studies on RIP transgenic mice have shown that several cytokines in addition to LT $\alpha$  and TNF (41, 42), including IL-2, IL-4, IL-6, IL-10, IFN- $\alpha$ , and IFN- $\gamma$ , induce pancreatic infiltrates (43). In addition, transgenic mice overexpressing IL-7 develop lymphoid infiltrates in the skin (44, 45). To test the possibility that cytokines might promote ectopic lymphoid tissue formation by inducing LT $\alpha$ 1 $\beta$ 2 expression on mature lymphocytes, we incubated splenocytes with various cytokines and measured staining of LT $\alpha$ 1 $\beta$ 2 with LT $\beta$ R-Fc. Strikingly, both IL-4 and IL-7 potently induced LT $\alpha$ 1 $\beta$ 2 expression on all naive (CD69<sup>-</sup>) CD4 and CD8 T cells (Fig. 7A) but not on B cells (data not shown). Titration analysis of IL-4 and IL-7 showed that 0.2–20 ng/ml of each cytokine was sufficient to trigger LT $\alpha$ 1 $\beta$ 2 induction (Fig. 7B). IL-15 induced LT $\alpha$ 1 $\beta$ 2 expression only on naive CD8 T cells but not CD4 T cells (Fig. 7A). The induction of LT $\alpha$ 1 $\beta$ 2 expression by these cytokines occurred independently of G $_i$ -coupled receptor signals, as it could not be blocked by pretreatment with Ptx (data not shown). A different pattern was observed for spontaneously activated CD4 and CD8 T cells (CD69<sup>+</sup>), as all IL-2 cytokine family members (IL-2, -4, -7, -15) were able to further enhance already elevated levels of surface LT $\alpha$ 1 $\beta$ 2 (data not shown), consistent with the up-regulation of the high-affinity receptor for IL-2 and IL-15 on activated T cells. All other cytokines tested at concentrations of 2–20 ng/ml, including IL-6, IL-10, IL-12, IFN- $\alpha$ , IFN- $\beta$ , IFN- $\gamma$ , and TNF, did not show any effect on LT $\alpha$ 1 $\beta$ 2 induction in 6-h cultures (data not shown). While these observations indicate that there must be several mechanisms that lead to ectopic lymphoid cell accumulation, they suggest that IL-4 and IL-7, and perhaps also IL-2, promote lymphoid tissue formation by activating the LT $\alpha$ 1 $\beta$ 2-LT $\beta$ R pathway.

## Discussion

The above findings demonstrate important differences among the three lymphoid tissue chemokines, CCL19, CCL21, and CXCL12, in their ability to recruit cells in vivo and promote ectopic lymphoid tissue formation. The two CCR7 ligands, CCL19 and CCL21, induce invasive infiltrates containing predominantly T and B cells and DCs. In contrast, the CXCR4 ligand, CXCL12, recruits

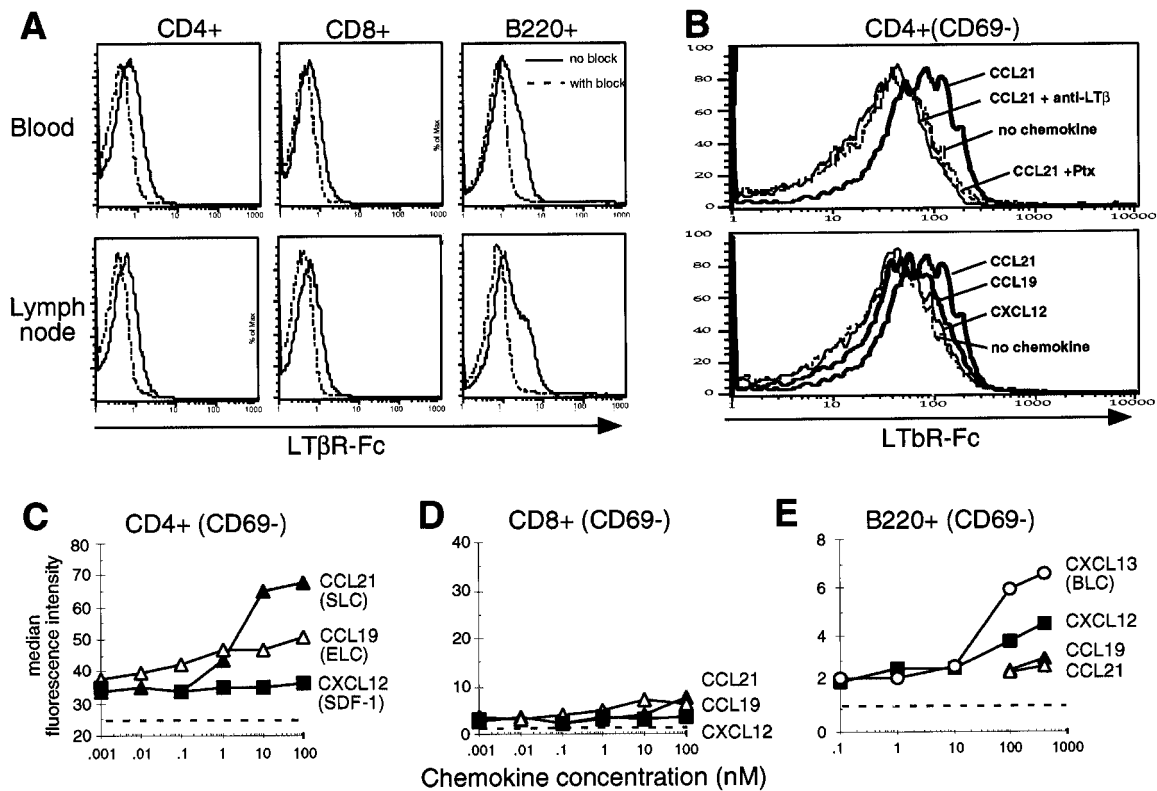


**FIGURE 5.** Membrane  $LT\alpha1\beta2$  expression by naive T cells and up-regulation by CCR7 signals. **A**, Naive T cells express detectable levels of membrane  $LT\alpha1\beta2$ . Flow cytometric analysis of cells from blood or lymph nodes stained for expression of  $LT\beta R$ -Fc on naive ( $CD69^{-}$ )  $CD4^{+}$ ,  $CD8^{+}$ , and  $B220^{+}$  cells. Solid lines show positive  $LT\beta R$ -Fc staining (no block) and dashed lines show  $LT\beta R$ -Fc staining in the presence of a  $LT\beta$  blocking Ab (with block). **B**, CCL19 and CCL21 induce  $LT\alpha1\beta2$  expression on naive T cells. Histograms show  $LT\beta R$ -Fc staining on gated naive ( $CD69^{-}$ )  $CD4^{+}$  splenocytes from in vitro cultures. Cells were incubated with 100 nM chemokines for 6 h with or without a 2-h preincubation with 200 ng/ml Ptx. *Upper panel*, Staining on cells incubated with medium (no chemokine), CCL21, or Ptx and CCL21. As a control, CCL21-treated cells stained in the presence of  $LT\beta$  blocking Ab are also shown. *Lower panel*, Cells incubated with 100 nM CCL21, CCL19, CXCL12, or no chemokine. **C–E**,  $LT\beta R$ -Fc staining on naive ( $CD69^{-}$ )  $CD4^{+}$ ,  $CD8^{+}$ , or  $B220^{+}$  cells after 6 h of incubation with CCL21, CCL19, CXCL12, or CXCL13 at the concentrations indicated. Data are presented as median fluorescence intensity of the  $LT\beta R$ -Fc signal obtained for the whole gated cell population. Dashed lines indicate the level of median fluorescence intensity when chemokine-treated cells were preincubated with anti- $LT\beta$  Ab. Data are representative of three chemokine titration experiments.

mainly B cells, DCs, and plasma cells. Each of the chemokines was sufficient to promote the appearance of markers of HEVs and lymphoid stromal cells, features associated with lymphoid neogenesis, although this was most prominent for CCL21. Importantly, CCL21 and CCL19 are shown to induce  $LT\alpha1\beta2$  up-regulation on naive  $CD4$  T cells. Furthermore, two cytokines that induce ectopic lymphoid tissue development, IL-4 and IL-7, were shown to be active in up-regulating  $LT\alpha1\beta2$  on naive  $CD4$  and  $CD8$  T cells. A third IL-2 family cytokine, IL-15, induced  $LT\alpha1\beta2$  on naive  $CD8$  T cells. These findings indicate that chemokine- and cytokine-mediated induction of  $LT\alpha1\beta2$  on naive T cells may participate in promoting development of endogenous and disease-associated lymphoid tissues.

In two previous studies, CCL21 expression in the pancreatic islets was observed to cause lymphoid neogenesis, with recruitment of lymphocytes and DCs, and development of HEVs and stromal cells (22, 23). Our findings in three RIP-CCL21 transgenic lines confirm the activity of CCL21 in promoting lymphoid neogenesis and extend these findings by demonstrating that  $LT\alpha1\beta2$  is required downstream of CCL21 for development of HEVs and stromal cells. Surprisingly, constitutive  $LT\alpha1\beta2$  does not appear to be needed for the presence of large numbers of lymphocytes in the islets, suggesting that many of the cells are present due to the direct recruiting activity of CCL21. It is also interesting that despite the greater chemotactic activity of CCL19 and CCL21 for T cells than

B cells, B cells often dominate the pancreatic infiltrates. It remains to be determined whether this effect is selective to the pancreas and whether factors in addition to the chemokines are involved.

Coexpression of CCL21 and CCL19 in lymphoid tissues is a conserved property between rodents and man, but the relative contribution of the two chemokines to leukocyte recruitment is unclear. In recent studies it was demonstrated that s.c. injection of CCL21 and CCL19 into *plt* mice, which lack lymphoid CCL19 and CCL21 protein, led to comparable T cell recruitment across HEVs in the draining lymph nodes (21, 46). However, our findings revealed strikingly lower amounts of CCL19 than CCL21 in lymph nodes and spleen of wild-type mice despite similar mRNA levels. Our estimates for CCL21 levels in lymph nodes and spleen, determined by Western blot, are comparable to the previously reported values determined by ELISA (22, 46). CCL19 protein levels have not been previously reported. Based on our measurements, and assuming a tissue density of 1 g/ml, we estimate CCL21 concentrations in total spleen and lymph node of 11,000–12,000 ng/ml and CCL19 concentrations of 20–40 ng/ml. As the T cell areas in spleen and lymph nodes correspond to only ~20–50% of the tissue area, the local chemokine concentrations within the T zone are likely to be severalfold higher than these estimates, with even higher concentrations at local points of production and secretion. Importantly, both of these concentration estimates are within ranges that have been found in vitro to induce chemotaxis of T cells and DCs (for examples, see Refs. 18, 47,



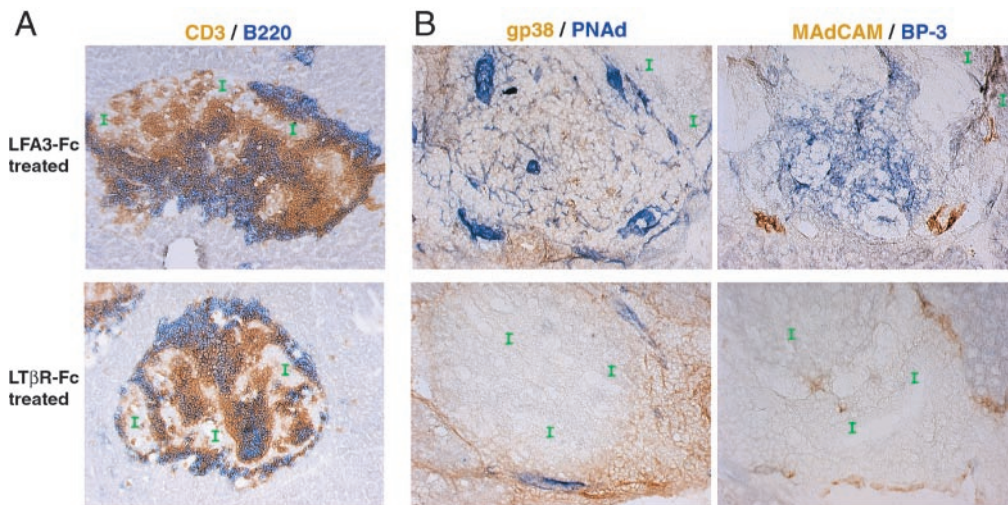


**FIGURE 6.** LT $\beta$ R-Fc treatment of RIP-CCL21 transgenic mice reduces expression of vascular addressins and the extent of the stromal cell network in pancreatic infiltrates. Immunohistochemical analysis of pancreatic sections from RIP-CCL21 mice treated for 20 days with LFA3-Fc (control) or LT $\beta$ R-Fc. *A*, Sections stained for CD3 in brown and B220 in blue, showing the small effect of LT $\beta$ R-Fc treatment on infiltrate size and T/B segregation. *B*, Staining for gp38 and MAdCAM in brown and PNAd and BP-3 in blue, as indicated, revealing a strong reduction in the extent of MAdCAM expression on HEVs and of gp38<sup>+</sup>, PNAd<sup>+</sup>, or BP-3<sup>+</sup> stromal cell networks in mice treated with LT $\beta$ R-Fc. I, Islet. Objective magnification:  $\times 10$  (*A*) and  $\times 20$  (*B*).

and 48). Previous studies have shown that the extended carboxyl-terminal domain of CCL21 contributes to increased retention of this protein in lymphoid tissue, probably because its highly basic properties favor interactions with extracellular proteoglycans (46). The absence of this domain in CCL19 may contribute to the poorer accumulation of the protein and might in turn indicate that CCL21 and CCL19 differ substantially in the extent and steepness of the chemoattractive gradients that they form. Our findings suggest that CCL21 will play a more important role in lymphoid tissue organization than CCL19.

Like CCL19 and CCL21, CXCL12 is a strong *in vitro* attractant of naive T cells (49). It is therefore significant that few T cells were recruited to the islets of RIP-CXCL12 transgenic mice. This may reflect insufficiency of CXCL12 for recruitment of T cells *in vivo*. The finding is also consistent with the possibility that CXCL12 has T cell chemorepellant activity (50). By contrast with the poor recruitment of T cells, CXCL12 caused notable accumulation of DCs, indicating that CXCL12 is sufficient to regulate the *in vivo* distribution of DCs. DCs are found near or within sites of endogenous CXCL12 expression, including the red pulp of the spleen (31) and in the gut and skin (32, 33, 51); therefore, we suggest that CXCR4 contributes to controlling DC positioning in both nonlymphoid and lymphoid tissues. The marked accumulation of plasma cells in RIP-CXCL12 transgenic islets is in agreement with the recent finding that CXCL12 is important in directing plasma cell movements *in vivo* (31) and indicates that CXCL12 is sufficient to cause accumulation of these cells. This observation suggests that the CXCL12 expressed in the joint synovium of rheumatoid arthritis patients (34, 35) contributes to the marked local accumulation of plasma cells that is typical of this disease (52).

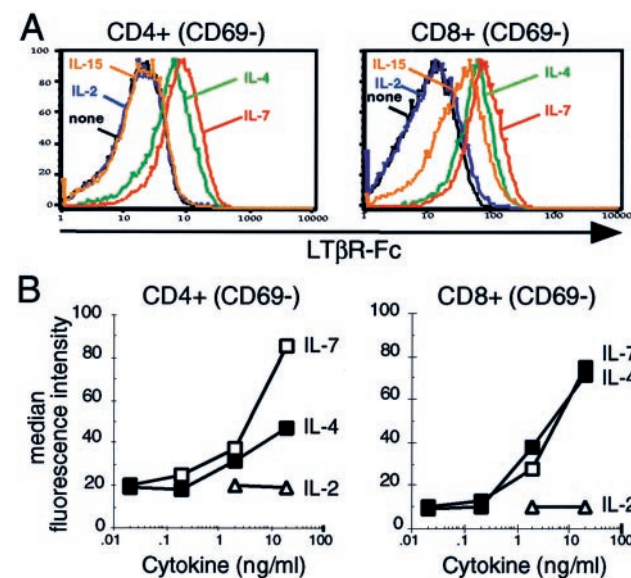


**FIGURE 7.** Cytokines IL-4, IL-7, and IL-15 induce LT $\alpha 1\beta 2$  expression on naive T cells. *A*, Histograms show LT $\beta$ R-Fc staining on naive (CD69<sup>-</sup>) CD4<sup>+</sup> or CD8<sup>+</sup> splenocytes from *in vitro* cultures. Cells were incubated for 6 h with 20 ng/ml IL-2, IL-4, IL-7, IL-15, or medium alone (none). Similar results were obtained from cultures incubated with the cytokines for 14 h (data not shown). *B*, LT $\beta$ R-Fc staining on naive (CD69<sup>-</sup>) CD4<sup>+</sup> or CD8<sup>+</sup> T cells after 14 h of incubation with IL-2, IL-4, or IL-7 at the concentrations indicated. Data are presented as median fluorescence intensity of the LT $\beta$ R-Fc signal obtained for the whole gated cell population.

LT $\alpha 1\beta 2$  expression has been reported previously on activated but not naive T cells (12, 53). We report low levels of LT $\beta$ R-Fc binding to naive T cells in blood and lymphoid tissues that can be blocked by an LT $\beta$ -specific Ab, suggesting low constitutive expression of LT $\alpha 1\beta 2$  on T cells. The physiological significance of LT $\alpha 1\beta 2$  expression by recirculating T cells remains to be determined, but it seems possible that it contributes to some aspects of lymphoid T zone organization. Compared with the low expression on naive T cells *ex vivo*, we find that CD4 T cells incubated *in vitro* with CCL21 or CCL19 express high levels of LT $\alpha 1\beta 2$ . The minimal induction on CD8 vs CD4 T cells is unexpected because both cell types respond similarly to CCL19 and CCL21 in chemotaxis assays and both up-regulate LT $\alpha 1\beta 2$  in response to IL-4 and IL-7. These observations suggest that different signaling pathways are activated by CCR7 within these two cell types. Interestingly, the activity of CCL19 and CCL21 in promoting LT $\alpha 1\beta 2$  expression on CD4 T cells was similar to or greater than the activity of CXCL13 in inducing expression on B cells (Fig. 5 and Ref. 8). *In vivo*, follicular CXCL13 up-regulates LT $\alpha 1\beta 2$  on naive B cells entering secondary lymphoid organs (8). However, we have not

observed differential  $LT\alpha1\beta2$  expression between naive T cells from blood vs spleen and lymph nodes. These observations appear paradoxical in the light of the 50- to 250-fold higher expression of CCL21 compared with CXCL13 within secondary lymphoid tissues, and suggest that  $LT\alpha1\beta2$  expression on naive CD4 T cells is negatively regulated within lymphoid tissue. It remains to be determined whether this is also the case at sites of inflammation.

Comparing the *in vitro* activities of CCL21 and CCL19 in  $LT\alpha1\beta2$  induction on CD4 T cells revealed that CCL21 was more effective than CCL19. In addition to the many studies that have shown  $LT\alpha1\beta2$  is necessary for lymph node and Peyer's patch development (10),  $LT\alpha$  expression has been shown to be sufficient to mediate lymphoid neogenesis in islets of transgenic mice (42). More recently, we demonstrated that development of organized infiltrates in response to ectopic CXCL13 was dependent on  $LT\alpha1\beta2$  (9). Therefore, the larger infiltrates induced by CCL21 compared with CCL19 may reflect the stronger induction of  $LT\alpha1\beta2$  by CCL21, in addition to the larger amounts of this chemokine present in the pancreas. CCL21-induced infiltrates have previously been shown to develop in the absence of B cells but not in the combined absence of T and B cells (22), supporting a role for T cell-derived  $LT\alpha1\beta2$  in promoting downstream effects in the infiltrate. Therefore, we propose that naive CD4 T cells attracted to the CCL21-expressing islets are induced to up-regulate  $LT\alpha1\beta2$ , leading to the development of HEVs and lymphoid stromal cells. Previous observations have shown an important role for  $LT\alpha1\beta2$  in the induction of CXCL13 and CCL21 and, to a lesser extent, CCL19 in secondary lymphoid tissues (54). The subsequent finding that CXCL13 could induce  $LT\alpha1\beta2$  on B cells led to the discovery of a positive feedback loop between  $LT\alpha1\beta2$  and CXCL13 (8). Although we have not been able to determine whether endogenous CCL21 is induced downstream of ectopically expressed CCL21, our findings are consistent with the possibility that CCL21 and  $LT\alpha1\beta2$  act together in a positive feedback loop. The possible pathological relevance of the relationship between CCL21 and  $LT\alpha1\beta2$  is supported by the finding of CCL21 mRNA (26) and protein (Fig. 2D) in the pancreatic infiltrates of NOD mice and the recent evidence that  $LT\alpha1\beta2$  is critical for development of diabetes in NOD mice (55, 56). It will be interesting in future studies to test whether blocking CCL21 function is sufficient to prevent development of diabetes in NOD mice.

The findings that chemokine-mediated ectopic lymphoid tissue formation correlated with the activity of chemokines in inducing  $LT\alpha1\beta2$  expression led us to ask whether cytokines that promote lymphoid infiltrates also induce  $LT\alpha1\beta2$  on naive lymphocytes. This inquiry revealed that IL-4, IL-7, and IL-15 were potent in up-regulating  $LT\alpha1\beta2$  expression *in vitro* on naive T cells, and all IL-2 cytokine family members promoted up-regulation on activated T cells. In this regard, it is significant that IL-4-induced infiltrates have been shown to contain MAdCAM-positive HEVs and stromal cells (43). Consistent with our observations, IL-2 has been shown to induce  $LT\alpha$  mRNA in spleen and lymph node cells (57). In other studies,  $LT\alpha$  has been characterized as a Th1 cytokine, and Gramaglia et al. (12) observed that Th2 cells do not express  $LT\alpha1\beta2$ , and combined IL-4 and anti-IFN- $\gamma$  treatment inhibited expression on activated T cells. We suspect that the differences between this latter study and our findings of  $LT\alpha1\beta2$  induction by IL-4 reflect that we treated freshly isolated splenocytes, whereas Gramaglia et al. (12) examined effects on TCR-activated cells. In other studies it has been shown that IL-7 up-regulates  $LT\alpha1\beta2$  on CD4<sup>+</sup>CD3<sup>-</sup>IL7R $\alpha$ <sup>+</sup> Peyer's patch-inducing cells (58). IL-7 is constitutively expressed within secondary lymphoid organs and is critical for survival of naive T cells (59–61). It is tempting to speculate that  $LT\alpha1\beta2$  induction on T cells by

IL-7 is part of the cross-talk occurring between recirculating T cells and  $LT\beta R$ - and IL-7-expressing T zone stromal cells. A general role of cytokine-mediated induction of  $LT\alpha1\beta2$  on naive lymphocytes may be to allow bystander cells to help reorganize tissue within the lymphoid organ or at a site of inflammation to better support the proliferation of the responding Ag-specific cells.

Finally, several recent studies have investigated the effect of lymphoid tissue chemokines on the antitumor immune response in mice. Introduction of CCL21 into the tumor caused increased infiltration by DCs, T cells, and in some cases granulocytes, and was associated with tumor regression (62–64). A comparison of the effects of transducing tumors with CCL19, CCL21, or CXCL12 in promoting tumor regression demonstrated that CCL21 was most effective, CXCL12 was intermediate, and CCL19 was least effective (65). Tumor targeting of LT was also recently shown to enhance T cell-mediated tumor regression (3). These combined observations agree well with our findings that CCL21 is highly effective in promoting T cell recruitment, LT up-regulation, and tissue invasion, and support further testing of this chemokine in antitumor immunotherapy.

## Acknowledgments

We thank Dr. Doug Hanahan (University of California, San Francisco, CA) for the RIP vector, Dr. Jeff Browning (Biogen) for  $LT\beta R$ -Fc and Ab (BBF6), and Drs. Jeff Browning and Richard Locksley for critical comments on the manuscript.

## References

- Lakkis, F. G., A. Arakelov, B. T. Konieczny, and Y. Inoue. 2000. Immunologic "ignorance" of vascularized organ transplants in the absence of secondary lymphoid tissue. *Nat. Med.* 6:686.
- Rennert, P. D., P. S. Hochman, R. A. Flavell, D. D. Chaplin, S. Jayaraman, J. L. Browning, and Y. X. Fu. 2001. Essential role of lymph nodes in contact hypersensitivity revealed in lymphotoxin- $\alpha$ -deficient mice. *J. Exp. Med.* 193:1227.
- Schrama, D., P. Thor Straten, W. H. Fischer, A. D. McLellan, E. B. Brocker, R. A. Reisfeld, and J. C. Becker. 2001. Targeting of lymphotoxin- $\alpha$  to the tumor elicits an efficient immune response associated with induction of peripheral lymphoid-like tissue. *Immunity* 14:111.
- Hjelmstrom, P. 2001. Lymphoid neogenesis: de novo formation of lymphoid tissue in chronic inflammation through expression of homing chemokines. *J. Leukocyte Biol.* 69:331.
- Cyster, J. G. 1999. Chemokines and cell migration in secondary lymphoid organs. *Science* 286:2098.
- Loetscher, P., B. Moser, and M. Baggiolini. 2000. Chemokines and their receptors in lymphocyte traffic and HIV infection. *Adv. Immunol.* 74:127.
- Zlotnik, A., J. Morales, and J. A. Hedrick. 1999. Recent advances in chemokines and chemokine receptors. *Crit. Rev. Immunol.* 19:1.
- Ansel, K. M., V. N. Ngo, P. L. Hyman, S. A. Luther, R. Förster, J. D. Sedgwick, J. L. Browning, M. Lipp, and J. G. Cyster. 2000. A chemokine driven positive feedback loop organizes lymphoid follicles. *Nature* 406:309.
- Luther, S. A., T. Lopez, W. Bai, D. Hanahan, and J. G. Cyster. 2000. BLC expression in pancreatic islets causes B cell recruitment and lymphotoxin-dependent lymphoid neogenesis. *Immunity* 12:471.
- Fu, Y.-X., and D. D. Chaplin. 1999. Development and maturation of secondary lymphoid tissues. *Annu. Rev. Immunol.* 17:399.
- Ware, C. F., T. L. VanArsdale, P. D. Crowe, and J. L. Browning. 1995. The ligands and receptors of the lymphotoxin system. *Curr. Top. Microbiol. Immunol.* 198:175.
- Gramaglia, I., D. N. Mauri, K. T. Miner, C. F. Ware, and M. Croft. 1999. Lymphotoxin  $\alpha\beta$  is expressed on recently activated naive and Th1-like CD4 cells but is down-regulated by IL-4 during Th2 differentiation. *J. Immunol.* 162:1333.
- Förster, R., A. E. Mattis, E. Kremmer, E. Wolf, G. Brem, and M. Lipp. 1996. A putative chemokine receptor, BLR1, directs B cell migration to defined lymphoid organs and specific anatomic compartments of the spleen. *Cell* 87:1037.
- Gunn, M. D., K. Tangemann, C. Tam, J. G. Cyster, S. D. Rosen, and L. T. Williams. 1998. A chemokine expressed in lymphoid high endothelial venules promotes the adhesion and chemotaxis of naive T lymphocytes. *Proc. Natl. Acad. Sci. USA* 95:258.
- Dieu, M. C., B. Vanbervliet, A. Vicari, J. M. Bridon, E. Oldham, S. Ait-Yahia, F. Briere, A. Zlotnik, S. Lebecque, and C. Caux. 1998. Selective recruitment of immature and mature dendritic cells by distinct chemokines expressed in different anatomic sites. *J. Exp. Med.* 188:373.
- Luther, S. A., H. L. Tang, P. L. Hyman, A. G. Farr, and J. G. Cyster. 2000. Coexpression of the chemokines ELC and SLC by T zone stromal cells and deletion of the ELC gene in the *plt/plt* mouse. *Proc. Natl. Acad. Sci. USA* 97:12694.
- Rossi, D. L., A. P. Vicari, K. Franz-Bacon, T. K. McClanahan, and A. Zlotnik. 1997. Identification through bioinformatics of two new macrophage proinflammatory human chemokines: MIP-3 $\alpha$  and MIP-3 $\beta$ . *J. Immunol.* 158:1033.



18. Ngo, V. N., H. L. Tang, and J. G. Cyster. 1998. Epstein-Barr virus-induced molecule 1 ligand chemokine is expressed by dendritic cells in lymphoid tissues and strongly attracts naive T cells and activated B cells. *J. Exp. Med.* 188:181.
19. Sallusto, F., B. Palermo, D. Lenig, M. Miettinen, S. Matikainen, I. Julkunen, R. Forster, R. Burgstahler, M. Lipp, and A. Lanzavecchia. 1999. Distinct patterns and kinetics of chemokine production regulate dendritic cell function. *Eur. J. Immunol.* 29:1617.
20. Vissers, J. L., F. C. Hartgers, E. Lindhout, M. B. Teunissen, C. G. Figdor, and G. J. Adema. 2001. Quantitative analysis of chemokine expression by dendritic cell subsets in vitro and in vivo. *J. Leukocyte Biol.* 69:785.
21. Baekkevold, E. S., T. Yamanaka, R. T. Palframan, H. S. Carlsen, F. P. Reinhold, U. H. von Andrian, P. Brandtzaeg, and G. Haraldsen. 2001. The CCR7 ligand efc (CCL19) is transcytosed in high endothelial venules and mediates T cell recruitment. *J. Exp. Med.* 193:1105.
22. Fan, L., C. R. Reilly, Y. Luo, M. E. Dorf, and D. Lo. 2000. Cutting edge: ectopic expression of the chemokine TCA4/SLC is sufficient to trigger lymphoid neogenesis. *J. Immunol.* 164:3955.
23. Chen, S. C., G. Vassileva, D. Kinsley, S. Holzmann, D. Manfra, M. T. Wiekowski, N. Romani, and S. A. Lira. 2002. Ectopic expression of the murine chemokines CCL21a and CCL21b induces the formation of lymph node-like structures in pancreas, but not skin, of transgenic mice. *J. Immunol.* 168:1001.
24. Reape, T. J., K. Rayner, C. D. Manning, A. N. Gee, M. S. Barnette, K. G. Burnand, and P. H. Groot. 1999. Expression and cellular localization of the CC chemokines PARC and ELC in human atherosclerotic plaques. *Am. J. Pathol.* 154:365.
25. Mazzucchelli, L., A. Blaser, A. Kappeler, P. Scharli, J. A. Laissue, M. Baggiolini, and M. Uguccioni. 1999. BCA-1 is highly expressed in *Helicobacter pylori*-induced mucosa-associated lymphoid tissue and gastric lymphoma. *J. Clin. Invest.* 104:R49.
26. Hjelmstrom, P., J. Fjell, T. Nakagawa, R. Sacca, C. A. Cuff, and N. H. Ruddle. 2000. Lymphoid tissue homing chemokines are expressed in chronic inflammation. *Am. J. Pathol.* 156:1133.
27. Takemura, S., A. Braun, C. Crowson, P. J. Kurtin, R. H. Cofield, W. M. O'Fallon, J. J. Goronzy, and C. M. Weyand. 2001. Lymphoid neogenesis in rheumatoid synovitis. *J. Immunol.* 167:1072.
28. Scheerens, H., E. Hessel, R. De Waal-Malefyt, M. W. Leach, and D. Rennick. 2001. Characterization of chemokines and chemokine receptors in two murine models of inflammatory bowel disease: IL10<sup>-/-</sup> mice and RAG2<sup>-/-</sup> mice reconstituted with CD4<sup>+</sup>CD45RB<sup>hi</sup> T cells. *Eur. J. Immunol.* 31:1465.
29. Yoneyama, H., K. Matsuno, Y. Zhang, M. Murai, M. Itakura, S. Ishikawa, G. Hasegawa, M. Naito, H. Asakura, and K. Matsushima. 2001. Regulation by chemokines of circulating dendritic cell precursors, and the formation of portal tract-associated lymphoid tissue, in a granulomatous liver disease. *J. Exp. Med.* 193:35.
30. Egawa, T., K. Kawabata, H. Kawamoto, K. Amada, R. Okamoto, N. Fujii, T. Kishimoto, Y. Katsura, and T. Nagasawa. 2001. The earliest stages of B cell development require a chemokine stromal cell-derived factor/pre-B cell growth-stimulating factor. *Immunity* 15:323.
31. Hargreaves, D. C., P. L. Hyman, T. T. Lu, V. N. Ngo, A. Bidgol, G. Suzuki, Y. R. Zou, D. R. Littman, and J. G. Cyster. 2001. A coordinated change in chemokine responsiveness guides plasma cell movements. *J. Exp. Med.* 194:45.
32. Casamayor-Palleja, M., P. Mondiere, A. Amara, C. Bella, M. C. Dieu-Nosjean, C. Caux, and T. DeFrance. 2001. Expression of macrophage inflammatory protein-3 $\alpha$ , stromal cell-derived factor-1, and B-cell-attracting chemokine-1 identifies the tonsil crypt as an attractive site for B cells. *Blood* 97:3992.
33. Pablos, J. L., A. Amara, A. Boulou, B. Santiago, A. Caruz, M. Galindo, T. Delaunay, J. L. Virelizier, and F. Arenzana-Seisdedos. 1999. Stromal-cell derived factor is expressed by dendritic cells and endothelium in human skin. *Am. J. Pathol.* 155:1577.
34. Buckley, C. D., N. Amft, P. F. Bradfield, D. Pilling, E. Ross, F. Arenzana-Seisdedos, A. Amara, S. J. Curnow, J. M. Lord, D. Scheel-Toellner, and M. Salmon. 2000. Persistent induction of the chemokine receptor CXCR4 by TGF- $\beta$ 1 on synovial T cells contributes to their accumulation within the rheumatoid synovium. *J. Immunol.* 165:3423.
35. Nanki, T., K. Hayashida, H. S. El-Gabalawy, S. Suson, K. Shi, H. J. Girschick, S. Yavuz, and P. E. Lipsky. 2000. Stromal cell-derived factor-1-CXC chemokine receptor 4 interactions play a central role in CD4<sup>+</sup> T cell accumulation in rheumatoid arthritis synovium. *J. Immunol.* 165:6590.
36. Hanahan, D. 1985. Heritable formation of pancreatic  $\beta$ -cell tumours in transgenic mice expressing recombinant insulin/simian virus 40 oncogenes. *Nature* 315:115.
37. Rennett, P. D., D. James, F. Mackay, J. L. Browning, and P. S. Hochman. 1998. Lymph node genesis is induced by signaling through the lymphotoxin  $\beta$  receptor. *Immunity* 9:71.
38. Gunn, M. D., S. Kyuwa, C. Tam, T. Kakiuchi, A. Matsuzawa, L. T. Williams, and H. Nakano. 1999. Mice lacking expression of secondary lymphoid organ chemokine have defects in lymphocyte homing and dendritic cell localization. *J. Exp. Med.* 189:451.
39. Vassileva, G., H. Soto, A. Zlotnik, H. Nakano, T. Kakiuchi, J. A. Hedrick, and S. A. Lira. 1999. The reduced expression of 6Ckine in the *plt* mouse results from the deletion of one of two 6Ckine genes. *J. Exp. Med.* 190:1183.
40. Kikutani, H., and S. Makino. 1992. The murine autoimmune diabetes model: NOD and related strains. *Adv. Immunol.* 51:285.
41. Picarella, D. E., A. Kratz, C. B. Li, N. H. Ruddle, and R. A. Flavell. 1993. Transgenic tumor necrosis factor (TNF)- $\alpha$  production in pancreatic islets leads to insulinitis, not diabetes: distinct patterns of inflammation in TNF- $\alpha$  and TNF- $\beta$  transgenic mice. *J. Immunol.* 150:4136.
42. Kratz, A., A. Campos-Neto, M. S. Hanson, and N. H. Ruddle. 1996. Chronic inflammation caused by lymphotoxin is lymphoid neogenesis. *J. Exp. Med.* 183:1461.
43. Mueller, R., T. Krahl, and N. Sarvetnick. 1997. Tissue-specific expression of interleukin-4 induces extracellular matrix accumulation and extravasation of B cells. *Lab. Invest.* 76:117.
44. Rich, B. E., J. Campos-Torres, R. I. Tepper, R. W. Moredith, and P. Leder. 1993. Cutaneous lymphoproliferation and lymphomas in interleukin 7 transgenic mice. *J. Exp. Med.* 177:305.
45. Watanabe, M., Y. Ueno, T. Yajima, S. Okamoto, T. Hayashi, M. Yamazaki, Y. Iwao, H. Ishii, S. Habu, M. Uehira, et al. 1998. Interleukin 7 transgenic mice develop chronic colitis with decreased interleukin 7 protein accumulation in the colonic mucosa. *J. Exp. Med.* 187:389.
46. Stein, J. V., A. Rot, Y. Luo, M. Narasimhaswamy, H. Nakano, M. D. Gunn, A. Matsuzawa, E. J. Quackenbush, M. E. Dorf, and U. H. von Andrian. 2000. The CC chemokine thymus-derived chemotactic agent 4 (TCA-4, secondary lymphoid tissue chemokine, 6Ckine, exodus-2) triggers lymphocyte function-associated antigen 1-mediated arrest of rolling T lymphocytes in peripheral lymph node high endothelial venules. *J. Exp. Med.* 191:61.
47. Campbell, J. J., E. P. Bowman, K. Murphy, K. R. Youngman, M. A. Siani, D. A. Thompson, L. Wu, A. Zlotnik, and E. C. Butcher. 1998. 6-C-kine (SLC), a lymphocyte adhesion-triggering chemokine expressed by high endothelium, is an agonist for the MIP-3 $\beta$  receptor CCR7. *J. Cell Biol.* 141:1053.
48. Yoshida, R., M. Nagira, T. Imai, M. Baba, S. Takagi, Y. Tabira, J. Akagi, H. Nomiyama, and O. Yoshie. 1998. EB11-ligand chemokine (ELC) attracts a broad spectrum of lymphocytes: activated T cells strongly up-regulate CCR7 and efficiently migrate toward ELC. *Int. Immunol.* 10:901.
49. Bleul, C. C., M. Farzan, H. Choe, C. Parolin, I. Clark-Lewis, J. Sodroski, and T. A. Springer. 1996. The lymphocyte chemoattractant SDF-1 is a ligand for LESTR/fusin and blocks HIV-1 entry. *Nature* 382:829.
50. Poznansky, M. C., I. T. Olszak, R. Foxall, R. H. Evans, A. D. Luster, and D. T. Scadden. 2000. Active movement of T cells away from a chemokine. *Nat. Med.* 6:543.
51. Agace, W. W., A. Amara, A. I. Roberts, J. L. Pablos, S. Thelen, M. Uguccioni, X. Y. Li, J. Marsal, F. Arenzana-Seisdedos, T. Delaunay, et al. 2000. Constitutive expression of stromal derived factor-1 by mucosal epithelia and its role in HIV transmission and propagation. *Curr. Biol.* 10:325.
52. Berek, C., and H. J. Kim. 1997. B-cell activation and development within chronically inflamed synovium in rheumatoid and reactive arthritis. *Semin. Immunol.* 9:261.
53. Ohshima, Y., L. P. Yang, M. N. Avicé, M. Kurimoto, T. Nakajima, M. Sergerie, C. E. Demeure, M. Sarfati, and G. Delespesse. 1999. Naive human CD4<sup>+</sup> T cells are a major source of lymphotoxin  $\alpha$ . *J. Immunol.* 162:3790.
54. Ngo, V. N., H. Korner, M. D. Gunn, K. N. Schmidt, D. S. Riminton, M. D. Cooper, J. L. Browning, J. D. Sedgwick, and J. G. Cyster. 1999. Lymphotoxin  $\alpha/\beta$  and tumor necrosis factor are required for stromal cell expression of homing chemokines in B and T cell areas of the spleen. *J. Exp. Med.* 189:403.
55. Ettinger, R., S. H. Munson, C. C. Chao, M. Vadeboncoeur, J. Toma, and H. O. McDevitt. 2001. A critical role for lymphotoxin- $\beta$  receptor in the development of diabetes in nonobese diabetic mice. *J. Exp. Med.* 193:1333.
56. Wu, Q., B. Salomon, M. Chen, Y. Wang, L. M. Hoffman, J. A. Bluestone, and Y. X. Fu. 2001. Reversal of spontaneous autoimmune insulinitis in nonobese diabetic mice by soluble lymphotoxin receptor. *J. Exp. Med.* 193:1327.
57. Reddy, J., P. Chastagner, L. Fiette, X. Liu, and J. Theze. 2001. IL-2-induced tumor necrosis factor (TNF)- $\beta$  expression: further analysis in the IL-2 knockout model, and comparison with TNF- $\alpha$ , lymphotoxin- $\beta$ , TNFR1 and TNFR2 modulation. *Int. Immunol.* 13:135.
58. Honda, K., H. Nakano, H. Yoshida, S. Nishikawa, P. Rennert, K. Ikuta, M. Tamechika, K. Yamaguchi, T. Fukumoto, T. Chiba, and S. I. Nishikawa. 2001. Molecular basis for hematopoietic/mesenchymal interaction during initiation of Peyer's patch organogenesis. *J. Exp. Med.* 193:621.
59. Schluns, K. S., W. C. Kieper, S. C. Jameson, and L. Lefrancois. 2000. Interleukin-7 mediates the homeostasis of naive and memory CD8 T cells in vivo. *Nat. Immunol.* 1:426.
60. Tan, J. T., E. Dudl, E. LeRoy, R. Murray, J. Sprent, K. I. Weinberg, and C. D. Surh. 2001. IL-7 is critical for homeostatic proliferation and survival of naive T cells. *Proc. Natl. Acad. Sci. USA* 98:8732.
61. Vivien, L., P. Benoist, and D. Mathis. 2001. T lymphocytes need IL-7 but not IL-4 or IL-6 to survive in vivo. *Int. Immunol.* 13:763.
62. Sharma, S., M. Stolina, J. Luo, R. M. Strieter, M. Burdick, L. X. Zhu, R. K. Batra, and S. M. Dubinett. 2000. Secondary lymphoid tissue chemokine mediates T cell-dependent antitumor responses in vivo. *J. Immunol.* 164:4558.
63. Kirk, C. J., D. Hartigan-O'Connor, B. J. Nickoloff, J. S. Chamberlain, M. Giedlin, L. Aukerman, and J. J. Mule. 2001. T cell-dependent antitumor immunity mediated by secondary lymphoid tissue chemokine: augmentation of dendritic cell-based immunotherapy. *Cancer Res.* 61:2062.
64. Vicari, A. P., S. Ait-Yahia, K. Chemin, A. Mueller, A. Zlotnik, and C. Caux. 2000. Antitumor effects of the mouse chemokine 6Ckine/SLC through angiostatic and immunological mechanisms. *J. Immunol.* 165:1992.
65. Nomura, T., H. Hasegawa, M. Kohno, M. Sasaki, and S. Fujita. 2001. Enhancement of anti-tumor immunity by tumor cells transfected with the secondary lymphoid tissue chemokine EBI-1-ligand chemokine and stromal cell-derived factor-1 $\alpha$  chemokine genes. *Int. J. Cancer* 91:597.